# Convex Hull Asymptotic Shape Evolution

Maxim Arnold, Yuliy Baryshnikov and Steven M. LaValle

University of Illinois, Urbana, IL 61801, USA; (MA: Institute for Information Transmission Problems, Moscow, Russia). Email: {mda,ymb,lavalle}@uiuc.edu

**Summary.** The asymptotic properties of Rapidly exploring Random Tree (RRT) growth in large spaces is studied both in simulation and analysis. The main phenomenon is that the convex hull of the RRT reliably evolves into an equilateral triangle when grown in a symmetric planar region (a disk). To characterize this and related phenomena from flocking and swarming, a family of dynamical systems based on incremental evolution in the space of shapes is introduced. Basins of attraction over the shape space explain why the number of hull vertices tends to reduce and the shape stabilizes to a regular polygon with no more than four vertices.

## 1 Introduction

Rapidly exploring Random Trees (RRTs) [11] have become increasingly popular as a way to explore high-dimensional spaces for problems in robotics, motion planning, virtual prototyping, computational biology, and other fields. The experimental successes of RRTs have stimulated interest in their theoretical properties. In [12], it was established that the vertex distribution converges in probability to the sampling distribution. It was also noted that there is a "Voronoi bias" in the tree growth because the probability that a vertex is selected is proportional to the volume of its Voronoi region. This causes aggressive exploration in the beginning, and gradual refinement until the region is uniformly covered. The RRT was generalized so that uniform random samples are replaced by any dense sequence to obtain deterministic convergence guarantees that drive dispersion (radius of the largest empty ball) to zero [13]. The lengths of RRT paths and their lack of optimality was studied in two recent works. Karaman and Frazzoli prove that RRTs are not asymptotically optimal and propose RRT*, which is a variant that asymptoticall yields optimal path lengths [6]. Nechushtan, Raveh and Halperin developed an automaton-based approach to analyzing cases that lead to poor path quality in RRTs [14]. More broadly, there has also been interest in characterizing convergence rates for other sampling-based planning algorithms that use random sampling [4, 5, 10].

In this paper, we address one of the long-standing questions regarding RRT behavior. Figure 1(a) shows how an RRT appears in a square region after 390 iterations.

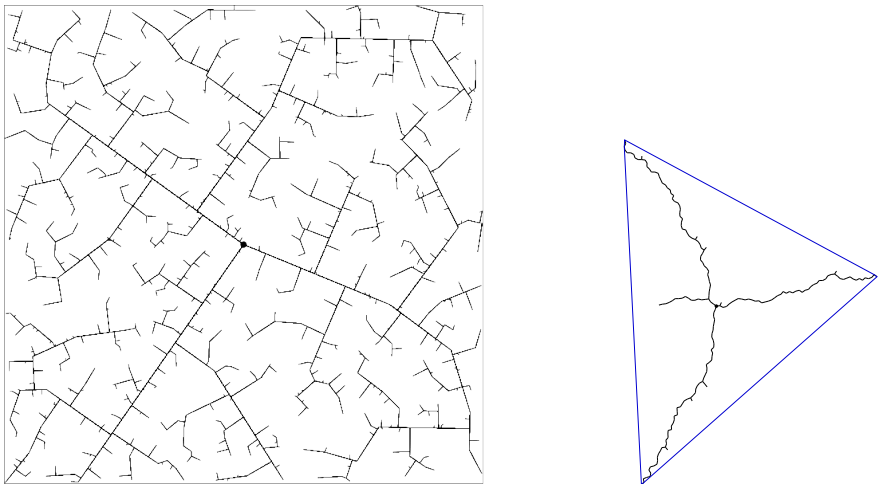

(a) (b)

**Fig. 1.** (a) An RRT after 390 iterations. (b) An RRT grown from the center of a "large" disc, shown with its convex hull.

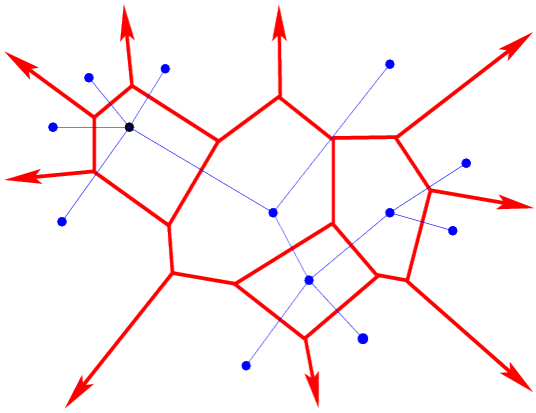

**Fig. 2.** The Voronoi diagram of RRT vertices contains interior Voronoi regions, which are bounded by other Voronoi regions, and exterior Voronoi regions, which extend to the boundary of the space.

What happens when the size of the search space is increased? In the limiting case in which an RRT sequence is generated in a large disc in the plane, simulations reliably produce three straight tree branches, roughly 120 degrees apart. See Figure 1(b). In terms of Voronoi bias, the exterior Voronoi regions completely dominate because the probability that random samples fall into interior Voronoi regions shrinks to zero; see Figure 2. Thus, the RRT spends virtually all of its time expanding, rather than refining in areas it has already explored.

It is remarkable that the convex hull of the RRT throughout the process is approximately an equilateral triangle with random initial orientation. This has been consistently observed through numerous simulations, and it known for over a decade with no rigorous analysis. How can this behavior be precisely characterized? Why does it occur? This motivates our introduction of *convex hull asymptotic shape evolution*, CHASE , which is a family of dynamical systems that includes the RRT phenomenon just described.

In addition to understanding RRTs, we believe that the study of CHASE dynamics encompasses a broader class of problems. Another, perhaps comparable in importance, motivation for our research comes from the general desire to understand self-organization in large, loosely interacting collectives of agents, whether natural or artificial. Although the literature on flocking, swarming, and general dynamics of large populations is immense, note that it is predominantly concentrated on *locally interacting* agents. Recently, a new trend has emerged, dealing with agents interacting over arbitrary distances. As examples, [16] deals with scale-invariant rendezvous protocols in swarms and naturalists provide us with the evidence that scale-invariant (*topological*, in their parlance) interactions exists in the animal world [2].

## 2 Dynamics of Shapes

### 2.1 Rapidly exploring trees

The *Rapidly exploring Random Tree* (RRT) is an incremental algorithm that fills a bounded, convex region $X \subset \mathbb{R}^d$ in the following way. Let $T(V,E)$ denote a rooted tree embedded in $X$ so that $V \subset X$ and every $e \in E$ is a line segment (with $e \subseteq X$). An infinite sequence $(T_0 \subset T_1 \subset T_2 \subset \ldots)$ of trees is constructed as follows. For $T_0(V_0,E_0)$, let $E_0 = \emptyset$ and $V_0 = \{x_{\texttt{root}}\}$ for any chosen $x_{\texttt{root}} \in X$, designated as the *root*. Each $T_i$ is then constructed from $T_{i-1}$. Let $\varepsilon > 0$ be a fixed *step size*. Select a point $x_{\texttt{rand}}$ uniformly at random in $X$ and let $x_{\texttt{near}}$ denote the nearest point in $T_{i-1}$ (in the union of all vertices and edges). If $x_{\texttt{near}} \in V_{i-1}$ and $\|x_{\texttt{near}} - x_{\texttt{rand}}\| \leq \varepsilon$, then $T_i$ is formed by $V_i := V_{i-1} \cup \{x_{\texttt{rand}}\}$ and $E_i := E_{i-1} \cup \{e_{\texttt{new}}\}$ in which $e_{\texttt{new}}$ is the segment that connects $x_{\texttt{near}}$ and $x_{\texttt{rand}}$. If $\|x_{\texttt{near}} - x_{\texttt{rand}}\| > \varepsilon$, then an edge of length $\varepsilon$ is formed instead, in the direction of $x_{\texttt{rand}}$, with $x_{\texttt{new}}$ as the leaf vertex. If $x_{\texttt{near}} \notin V_{i-1}$, then it must appear in the interior of some edge $e \in E$. In this case, $e$ is split so that both of its endpoints connect to $x_{\texttt{near}}$. Recall Figure 1(a), which shows a sample RRT for $X = [0,1]^2$. The RRT described here uses the entire swath for selection, rather than vertices alone, as described in [11]. For a discussion of how

these two variants are related, see [13]; the asymptotic phenomena are independent of this distinction.

### 2.2 An isotropic process

Consider the case in which the starting point $x_{\texttt{root}}$ is at the origin, and the region to be explored (and the sampling density) is *rotationally invariant*. In the limit of small $\varepsilon$, the RRT growth is governed by the direction towards the $x_{\texttt{rand}}$ (far away), which can be assumed to be uniformly distributed on the unit circle or directions. In this case, the dynamics of the *convex hulls* of the successive RRTs can be described as follows.

Let $\mathbf{P}_n$ denote the convex hull of the points $x_1,\dots,x_n \in \mathbb{R}^2$. The random polygon $\mathbf{P}_{n+1}$ depends on $x_1,\dots,x_n$ only through $\mathbf{P}_n$ via the following iterative process:

**Algorithm 1** Dynamics of the convex hulls of early RRTs in the limit of small step sizes.

$n \leftarrow 0, \mathbf{P}_0 \leftarrow \mathbf{0}$
**loop**
  $l \leftarrow \texttt{rand}(S^1)$
  $v \leftarrow \texttt{argmax}\langle l, x\rangle, x \in \mathbf{P}_n$
  $\mathbf{P}_{n+1} \leftarrow \texttt{conv}(\mathbf{P}_n \cup \{v + \varepsilon l\})$
  $n \leftarrow n+1$
**end loop**

This algorithm defines an increasing family of (random) convex polygons. One might view it as a (growing) Markov process on the space of convex polygons in $\mathbb{R}^2$ starting with the origin $\mathbf{P}_0$.

Note that as the Markov chain evolves, the number of vertices in $\mathbf{P}_n$ can change. Some vertices can disappear, being swept over by the convex hull of the newly added point. This new point does not eliminate the vertex $v_l$, where the functional $\langle \cdot, l\rangle$ attains its maximum if and only if the vector $-l$ does not belong to the cone $T_{v_l^n}\mathbf{P}_n$, the tangent cone to $\mathbf{P}_n$ at $v_l$. This, in turn, can happen only if the angle at $v_l$ is acute (less than $\pi/2$).

#### The enigma of the symmetry breaking

Although the distribution of this growth process is manifestly rotationally invariant, our simulations show that after long enough time the polygons $\mathbf{P}_n$ are not becoming round. On the contrary, it was observed that the polygons $\mathbf{P}_n$ become close (in *Hausdorff metric*[1]) to large equilateral triangles. (It should be noted that the polygons are

[1] A Hausdorff metric between two compact subsets of a metric space can be defined as $d_H(A,B) = \max_{a\in A}\min_{b\in B} d(a,b) + \max_{b\in B}\min_{a\in A} d(a,b)$.

actually triangles only for a fraction of the time; typically some highly degenerate - with an interior angle close to $\pi$ - vertices are present.)

Although we still do not understand completely the mechanisms of symmetry breakage and of the formation of the asymptotic shapes, there are several asymptotic results and heuristic models that shed enough light on the process to at least make plausible explanations of the observed dynamics. This paper addresses with these results and models.

### 2.3 Sources of difficulties

The biggest problem emerging when one attempts to analyze the Markov process $\{\mathbf{P}_n\}_{n=1,2,\ldots}$ is the lack of a natural parameterization of the space of the polygons: An attempt to account for all convex planar polygons at once leads immediately to an infinite dimensional (and notoriously complicated) space of convex support functions (with $C^0$ norm-induced topology). Indeed, starting with any polygon, the Markov process will have a transition, with positive probability, changing the collection of vertices forming the convex polygon $\mathbf{P}_n$.

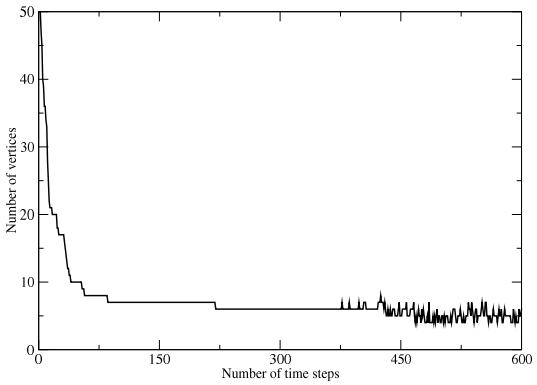


**Fig. 3.** Typical behavior of the number of vertices of $\mathbf{P}_n$, starting with a regular 50-sided polygon.

While the experimental evidence suggests that the polygons $\mathbf{P}_n$ become close to equilateral triangles in Hausdorff metric, there is little hope to understand the process of the *vertices* of $\mathbf{P}_n$ because even the number of vertices changes with high frequently (see Fig. 3)

### 2.4 Outline of the results

For the reason above, we adopt a circumvential route here. In lieu of addressing the complicated dynamics defined by Algorithm 1 throughout, we concentrate here on the time intervals over which the number of the vertices of $\mathbf{P}_n$ remains constant. During each such interval, the evolution of the convex polygons $\mathbf{P}$ can be described as a relatively straightforward (time-homogeneous) Markov process on the space of the $k$-sided polygons.

*If* the number of vertices of polygons $\mathbf{P}_n$ were to stabilize, then the size (perimeter) of these polygons would grow linearly in time. This suggests considering a Markov process on the space of *shapes* of $k$-sided polygons. To obtain a *shape* from the original polygon one could fix a direction of the one of the sides and scale the whole polygon to have a fixed circumference. To be consistent one should apply the same scaling also on the incremental steps of the original Markov process. We define the state space of this new process, which is the space of shapes of $k$-sided polygons, in Section 2.5).

Since increments of the new process are scaled at each time-step of the algorithm, it cannot be time-homogeneous anymore. Since size of the original polygon grows linearly with time we approximate scaled process on the space of shapes by the similar one with the increments exactly of size $1/n$.

Markov processes with diminishing step sizes are quite familiar in the theory of stochastic approximation, where we represent the Markov process as a shift along a vector field (obtained by the *averaging*) perturbed by small random noise.

We will describe this averaged dynamical system (which we will refer to as CHASE, for Convex Hull Asymptotic Shape Evolution) in Section 3. Interestingly, it can be interpreted (up to a time reparameterization) as the gradient field for the circumference of the polygonal chain(see proposition 2 for the details): CHASE dynamics tries to make the polygonal chain longer the fastest way!

It is well known that for small steps, the stochastically perturbed processes are tracing closely their deterministic, averaged counterparts for long times. More to the point, classical results (see [9, 15]) on stochastic approximations imply that *perturbed dynamical system remains trapped with probability one near an exponentially stable equilibrium of the averaged dynamics*, if deviations of the stochastic perturbation scale such as $1/n$ (or any other scale $\varepsilon_n$ such that $\sum \varepsilon_n = \infty$ and $\sum \varepsilon_n^2 < \infty$).

Thus, the first natural step to try to explain the lack of polygonal shapes other than equilateral triangles in the long runs of $\mathbf{P}_n$ would be to analyze the averaged dynamics of our scaled Markov processes on the polygonal chains, locating their equilibria and studying their stability.

As it turned out, for $k$-sided polygonal chains, the only nondegenerate fixed points of CHASE are the regular polygons [2]. Moreover, we prove that these equilibria are unstable for $k \geqslant 5$.

Our averaging procedure hardly relies on the fact that the number of vertices of the polygon (equivalently, the dimension of the corresponding space of shapes)

[2] CHASE can be extended to non-convex polygons; the regular polygons therefore can be non-convex ones as well.

remains fixed. Thus, for $k$-sided polygons with obtuse internal angles, the scaled Markov chain $\mathbf{P}_n$ is well-approximated by CHASE. In general, for polygons with acute internal angles, $\mathbf{P}_n$ has non-zero probability of changing the number of vertices. From that it follows that an averaging procedure cannot be applied without modifications for the triangles and quadrangles. However we strongly believe that one can modify the averaging procedure in such a way, that generalized CHASE dynamics could be extended to that cases. In Section 4.5 we present some results that heuristically lend support to the natural conjecture that the regular triangles are stable shapes under any generalized averaged dynamics.

We conclude the paper with a short description of limit of CHASE for the obtuse $k$-sided polygons, as $k \to \infty$.

### 2.5 A space of shapes

We begin with the formal description of the space of shapes.

#### The construction

A *configuration* of $k$ points (or *k-configuration*) is a collection of distinguishable (uniquely labeled) points in $\mathbb{R}^2$, not all coincident. Traditionally, the *shape* of a configuration is understood as its class under the equivalence relation on the configurations defined by the Euclidean motions and the change of scale. More specifically, two configurations $\{x_1,\dots,x_k\}$ and $\{x'_1,\dots,x'_k\}$ are said to have the same shape if there exists some rotation $U \in SO(2)$, translation vector $v \in \mathbb{R}^2$ and scaling constant $\lambda > 0$ so that $x'_i = \lambda U x_i + v$ for all $i$ from 1 to $k$. Factorings by the scale and the displacement admit sections: One can assume that the center of gravity of the configuration is at the origin and its moment of inertia is 1 (or that $\sum_i |x_i|^2 = 1$) – this is where the condition that not all points coincide is important. For a natural interpretation of the space shape in terms of symplectic reduction, see [8].

#### Complex projective spaces

Perhaps most explicit way to think about the space of shapes of planar $k$-configurations is the following: Viewing $\mathbb{R}^2$ as $\mathbb{C}$, we can interpret the $k$-configuration with the center of mass at the origin as a point in $\mathbb{C}^{k-1} - \{0\}$. Factoring by rotations and rescaling is equivalent to factoring by $\mathbb{C}_*$, the multiplicative group of complex numbers, whence the space of shapes is isomorphic (as a Riemannian manifold) to $\mathbb{CP}^{k-2}$, the $(k-2)$-dimensional complex projective space.

The simplest nontrivial case $k = 3$ is very instructive: $\mathbb{CP}^1$ is isometric to the Riemannian sphere $S^2$. The poles of the sphere can be identified with the equilateral triangles (North or South depending on the orientation defined by the cyclic order of $x_1, x_2, x_3$); the equator corresponds to the collinear triples, and the parallels to the level sets of the (algebraic) area, considered as the function of the configurations rescaled to unit moment of inertia (see Figure 4). For related shape space constructions, see [7] and an application to robotics in which probability mass is placed over the shape space [3].

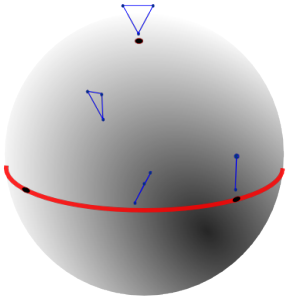

**Fig. 4.** The sphere of shapes of triangles. The equator consists of degenerate triangles (three points collinear). The poles correspond to equilateral triangles.

### Tame configurations and the $k$-gon dynamics

The space of planar $k$-configurations contains an open subset consisting of *tame* ones, which we define here as the configurations for which every two consecutive sides form a positively oriented frame (in particular, meaning all points of the configuration are distinct) and the angle between these vectors is acute:

$$(x_i - x_{i-1}) \times (x_{i+1} - x_i) > 0 \text{ and } (x_i - x_{i-1}) \cdot (x_{i+1} - x_i) > 0,$$

assuming modular indexing. The space of tame configurations is invariant with respect to rotations and dilatations, and its image in the shape space $\mathtt{conf}_k = \mathbb{CP}^{k-2}$ is an open contractible set (for $k = 3$ it is the upper hemisphere of $S^2$). We will denote both the space of tame $k$-configurations and the corresponding subset of the shape space as $\mathtt{conf}_k^+$.

Note that if $\mathbf{P}_n \in \mathtt{conf}_k^+$, then there exists a step size $\varepsilon$ small enough so that $\mathbf{P}_{n+1} \in \mathtt{conf}_k^+$. Equivalently, the Markov dynamics on sufficiently large and tame configurations preserves tameness, for at least a while.

Define the *tamed Markov process* $\mathbf{P}_n^{(k)}$ by the algorithm:

**Algorithm 2** Tamed dynamics.

$n \leftarrow 0, \mathbf{P}_0^{(k)} = (v_1, \ldots, v_k) \in \mathtt{conf}_k$
**loop**
  $l \leftarrow \mathtt{rand}(S^1)$
  $i \leftarrow \mathtt{argmax}\langle l, v_i \rangle, v_i \in \mathbf{P}_n^{(k)}$
  $v_i \leftarrow v_i + \varepsilon l$
  $n \leftarrow n + 1$
**end loop**

Algorithm 2 is just a formal generalisation of Algorithm 1 to the space of tamed configurations. While the resulting dynamics is different one can still notice that

Markov processes $\mathbf{P}_n$ and $\mathbf{P}_n^{(k)}$ are coupled on tame configurations. As one of our goals is to *disprove* that the Markov process $\mathbf{P}_n$ can ever converge to a $k \geqslant 5$-sided polygon, it is sufficient to disprove this for $\mathbf{P}_n^{(k)}$.

## 3 Tamed Dynamics

The tamed Markov process possesses several features that simplify its treatment considerably, compared to the original Markov process. First and foremost, the tamed dynamics stays in the space of $k$-sided polygonal chains, isomorphic to $\mathbb{R}^{2k}$. Furthermore, the fact that the number of the "growth points" is bounded directly implies that the size of the polygonal chain grows with $\Theta(t)$.

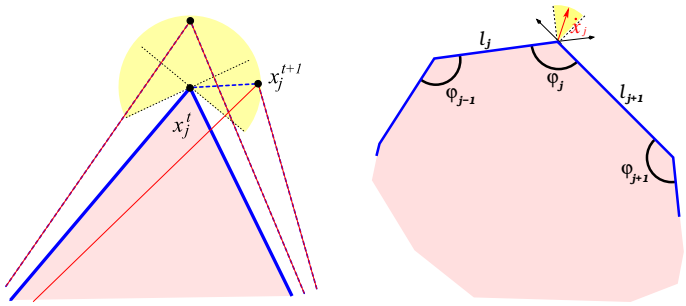


**Fig. 5.** The original dynamics of the RRT convex hulls and tamed dynamics coincide for any obtuse angle and are coupled for small enough increments for acute enough angles. (a) Tamed dynamics (in red) versus original dynamics (dashed blue). (b) For obtuse angles, the cone of possible directions (yellow) is spanned by the lines $(x_j - x_{j-1})^\perp$ and $(x_{j+1} - x_j)^\perp$.

Denote by $\psi(\mathbf{P})$ the perimeter of the (not necessarily convex) polygon $\mathbf{P}$.

**Lemma 1** *The expected perimeter of* $\mathbf{P}^{(k)}$ *grows linearly: There exists some* $c, C > 0$ *for which*

$$\mathbb{P}\left(\psi(\mathbf{P}^{(k)}{}_n) < cn\right) \leq \exp(-Ct).$$

(Note that a linear upper bound on the perimeter of $\mathbf{P}^{(k)}{}_n$ and of $\mathbf{P}_n$ is immediate.)

### 3.1 Continuous dynamics

The stochastic process $\mathbf{P}^{(k)}$ can be viewed as a deterministic flow on the space $V_{\mathbf{P}}^k$ of $k$-sided polygons, subject to small noise. Indeed, by Lemma 1, the size of the polygons $\mathbf{P}^{(k)}$ grows linearly while the relative size of the steps decreases.

Given a polygonal $k$-chain $\mathbf{P}$, consider the expected increment

$$\Delta\mathbf{P} := \mathbb{E}({\mathbf{P}^{(k)}}_{n+1}|{\mathbf{P}^{(k)}}_n = \mathbf{P}) - \mathbf{P}$$

(we use here the linear structure on $V^k_{\mathbf{P}}$). The following is immediate:

**Lemma 2** *The function $\Delta$ commutes with rotations and is homogeneous of degree* 0.

The linear growth of the sizes of polygons $\mathbf{P}^{(k)}$ together with the homogeneity of $\Delta$ indicate that asymptotically, the expected increments are small compared to the size of $\mathbf{P}^{(k)}$. In such a situation, an approximation of the discrete stochastic dynamics by a continuous deterministic one is a natural step. This motivates the following

**Definition 1** *The vector field*

$$\dot{\mathbf{P}} = \Delta\mathbf{P}$$

*on $V^k_{\mathbf{P}}$ is called the* CHASE *dynamics.*

In coordinates, the CHASE dynamics is given as follows (see Fig 5b):

**Corollary 1** *Assume that* $\mathbf{P}$ *consists of the vertices* $(x_1,\dots,x_k)$, $x_i \in \mathbb{R}^2$ *in cyclic order, and* $(x_{i_1}, x_{i_2}, \dots, x_{i_c})$ *are the vertices of* $\mathbf{P}$ *on its convex hull. Then*

$$\dot{x}_{i_l} = \frac{x_{i_l} - x_{i_{l+1}}}{|x_{i_l} - x_{i_{l+1}}|} + \frac{x_{i_l} - x_{i_{l-1}}}{|x_{i_l} - x_{i_{l-1}}|}, \tag{1}$$

*and $\dot{x}_i = 0$ if $x_i$ is not on the convex hull of* $\mathbf{P}$.

### 3.2 Theorem: The discrete-time process converges to the continuous-time system

The intuitive proximity of the $\mathbf{P}^{(k)}$ dynamics and the trajectories of CHASE flow can be made rigorous, using some standard tools. Specifically, we have shown:

**Theorem 1** *Let* $\mathbf{P} \in V^k_{\mathbf{P}}$, *and* ${\mathbf{P}^{(k)}}_n, 0 \le t \le C\lambda$ *be the (random) trajectory of the tamed Markov dynamics with the initial configuration* $\lambda\mathbf{P}$. *Similarly, let* $\mathbf{P}(n), 0 \le n \le \lambda^C$ *be the trajectory of the* CHASE *dynamics starting with the same initial point* $\lambda\mathbf{P}$. *Then for any $C > 0$, the trajectory* ${\mathbf{P}^{(k)}}_n/\lambda$ *converges to* $\mathbf{P}(n)/\lambda$ *in probability in $C_0$ norm, as $\lambda \to \infty$.*

The proof requires some relatively extensive setup and will not be presented here. However, it is conceptually transparent: The deviations of the stochastic dynamics from the continuous one has linearly growing quadratic variations, and, by martingale large deviation results (using, for example, Azuma's inequality), one can prove the proximity of the trajectories for times of order $\lambda$, with probability exponentially close to 1. In other words, the shape of the tamed process follows the CHASE dynamical system.

The approach is close to many classical treatments of stochastically perturbed dynamical systems, see e.g.[9]. It should be noted that *if one rescales* the polygons $\mathbf{P}^{(k)}$ by $n$ (to keep their linear sizes approximately constant), then the step sizes become $c/n$, which is the typical scale of the algorithms of stochastic approximation (compare to [15]).

# 4 Properties of CHASE Flow.

We outline several properties of the CHASE dynamics and then analyze their equilibria.

## 4.1 Symmetries

High symmetries is one of the attractive features of the CHASE dynamics. Lemma 2 implies:

**Proposition 1** *The* CHASE *dynamics defines a field of directions (a vector field defined up to point-dependent rescaling) on the shape space* $V^k_{\mathbf{P}}$.

(We will be retaining the name for the field of direction on $V^k_{\mathbf{P}}$ obtained by the projection of CHASE .)

This means that we can track track the shapes in $V^k_{\mathbf{P}}$. In particular, if there would exist an exponentially stable critical point of the reduction of the CHASE dynamics to the shape space, then the tamed process would have a positive probability of converging to the corresponding shape. However, as we will show below, there are no stable equilibria in the space $V^k_{\mathbf{P}}$ for $k \geqslant 5$.

## 4.2 CHASE is the gradient flow.

Another interesting property of CHASE is the fact that it is a *gradient* flow, with respect to the natural Euclidean metric on $V^k_{\mathbf{P}}$:

**Proposition 2** *The* CHASE *dynamics is the gradient of the function* $\psi(\mathbf{P})$ *taking a polygonal chain to the perimeter of its convex hull.*

The proof is direct: The variation of the length of the side $[x_{i_l}, x_{i_{l+1}}]$, if $x_{i_l}$ changes infinitesimally, is the scalar product with

$$\frac{x_{i_l} - x_{i_{i+1}}}{|x_{i_l} - x_{i_{i+1}}|};$$

therefore, the claim follows.

Note that if one chooses the *other bisector*

$$\dot{x}_{i_l} = \frac{x_{i_l} - x_{i_{i+1}}}{|x_{i_l} - x_{i_{i+1}}|} - \frac{x_{i_l} - x_{i_{i-1}}}{|x_{i_l} - x_{i_{i-1}}|}, \tag{2}$$

as the direction of the velocity, then the resulting dynamics would *preserve* the perimeter and is useful in building customized Birkhoff's billiard tables; see [1].

### 4.3 Equilibria

According to Proposition 1, CHASE defines a vector field on $V^k_{\mathbf{P}}$, and one would like to understand which shapes are preserved by these dynamics. Clearly, the *regular* $k$-polygons are preserved. Three more classes of shapes are preserved as well (see Figure 6): Trapezoids, rhombi, and *drops*, which are obtained from a regular $2k$-polygon by extending a pair of next-to-opposite sides.

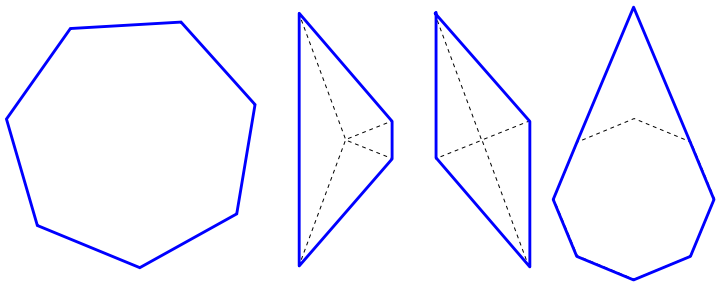

**Fig. 6.** From left to right, the only shapes preserved by the CHASE dynamics: regular polygons, trapezoids, rhombi, and drops. For the rhombus and trapezoid, the dashed lines show the bisectors.

As it turned out, these classes exhaust all possible shapes that are invariant under the CHASE dynamics:

**Theorem 2** *The equilibrium points of* CHASE *in* `conf` *consist of the polygonal chains for which their convex hulls (having $i \le k$ vertices) are regular $i$-sided polygons.*

*Proof.* Via straightforward trigonometry (using the notation shown in Figure 5b), we derive the rate of change of the angle $\varphi_j$ as given by

$$\dot{\varphi}_j = \frac{\sin\varphi_{j+1} - \sin\varphi_j}{\ell_j} + \frac{\sin\varphi_{j-1} - \sin\varphi_j}{\ell_{j-1}}, \tag{3}$$

and, similarly, the rates for the lengths $\ell_j$:

$$\dot{\ell_j} = 2 + \cos\varphi_j + \cos\varphi_{j-1}. \tag{4}$$

If the shape of the polygon remains invariant, then the angles are constant. This implies a system of linear equations on $s_j := \sin\varphi_j$'s. It is immediate that this system is identical to the conditions on stationary probabilities on a continuous time Markov chain on the circular graph with transition rates $1/\ell_j$. As this auxiliary Markov chain is manifestly ergodic, such stationary probabilities are unique and therefore the solutions are spanned by the vectors of $(s_j)_j = (1,1,\ldots,1)$. Hence, all $\sin\varphi_j$ are equal, and that therefore for some $\varphi$, all of $\varphi_j$ are equal to either $\varphi$ or $\pi - \varphi$.

Note that this condition implies that one of the following holds: 1) There are three acute angles, forcing the polygon to be a regular triangle; 2) there are two acute angles equal to $\varphi < \pi/2$, and two complementary angles of $\pi - \varphi$, forcing the polygon to be either a trapezoid or a rhombus; 3) there is one acute angle $\varphi$, and all the remaining angles are equal to $\pi - \varphi$; 4) all angles are obtuse.

Quadrangles are realizable with the angle $\varphi$ being a continuous shape parameter. For the last two cases, the preservation of the shape implies that the ratios of the lengths $\ell_j/\ell_{j+1}$ remains constant, and therefore equal to the ratios of $\dot{\ell}_j/\dot{\ell}_{j+1}$. Combining this with (4) implies that the ratios of the lengths $\ell_i/\ell_j$ can take only the following values (in the case of one acute angle):

$$1, \frac{1 \mp \cos\varphi}{1 \pm \cos\varphi}, (1 \pm \cos\varphi)^{\pm 1}.$$

This immediately leads to the conclusion that only the drop shape can satisfy this condition.

For the case in which all the angles are equal, the equality of all side lengths is obvious. □

### 4.4 Regular polygons are unstable

As discussed in Section 2.5, the space of shapes of $k$-sided polygonal chains is naturally isomorphic to $k-2$-dimensional complex projective space and has therefore (real) dimension $2k-4$.

A natural coordinate frame on a (everywhere dense) chart in this space is given by *the lengths of the sides* of the $k$-gon, normalized to $\sum \ell_j = 1$ (this gives $k-1$ coordinates) and the collection of angles $\varphi_j$ satisfying the condition $\sum \varphi_j = (k-2)\pi$. The condition of closing the polygon implies that only $(k-3)$ of these angles are independent.

Under the CHASE dynamics, the vertices of the $k$-sided polygon move according to (2). The next theorem establishes that the regular $k$-sided polygon, although a fixed point of CHASE dynamics, is *unstable* in the linear approximation.

Note that the vector field on the shape space is defined only up to multiplication by a positive smooth function. However, one can readily verify that the linearization of the vector field at an equilibrium point is unaffected by this ambiguity.

**Theorem 3** *For the linearization of the* CHASE *dynamics near the $k$-regular polygonal chain, the $2k-4$-dimensional space of $k$-sided shapes has exactly one $(k-3)$-dimensional stable subspace (tangent to the manifold $\{\varphi = \text{const}\}$ and one $(k-1)$-dimensional invariant subspace, unstable for $k \geqslant 5$.*

*Proof.* One can check immediately that under the CHASE evolution, the sides of the $k$-gons with all angles equal (to $\pi(1-2/k)$) move parallel to themselves. This proves the invariance of $\{\varphi = \text{const}\}$ and also the fact that (when considered in the space of $k$-sided polygons) the lengths are all growing linearly with the same speed. Therefore, their ratios asymptotically tend to 1, proving the first claim.

It follows that in the $(\ell, \varphi)$ frame on `conf`, the linearization of the CHASE vector field is block-upper-triangular:

$$J = \begin{pmatrix} J_\ell & * \\ 0 & J_\varphi \end{pmatrix}$$

. Using (3) we compute $J_\varphi$, to obtain a cyclic tri-diagonal matrix:

$$J_\varphi = -\frac{2\cos(\frac{(k-2)\pi}{k})}{\ell} \begin{pmatrix} 2 & -1 & 0 & \cdots & 0 & -1 \\ -1 & 2 & -1 & 0 & \cdots & 0 \\ 0 & -1 & 2 & -1 & \cdots & 0 \\ \vdots & & \ddots & \ddots & \ddots & \vdots \\ 0 & \cdots & 0 & -1 & 2 & -1 \\ -1 & 0 & \cdots & 0 & -1 & 2 \end{pmatrix};$$

therefore,

$$\operatorname{spec}(J_\varphi)_j = -\frac{4\cos(\frac{(k-2)\pi}{k})}{\ell} \left(1 - \cos\left(\frac{2\pi j}{k}\right)\right),$$

which belongs to $(0, \infty)$ if $k \geqslant 5$. This proves the claim. □

### 4.5 Stability of triangles

A corollary of the proof of Theorem 3 implies that the regular triangles, under the CHASE dynamics, are stable. This result is, however, relatively irrelevant, because the Markov chain $\mathbf{P}_n$ is rather different from the tamed dynamics (which is approximated by CHASE ): the triangles acquire extra vertices, and, although the growth of the resulting polygons might or might not be slowed down compared to the tamed process, we are currently unable to analyze it.

For this reason we present a simple analysis that is somewhat more general than CHASE dynamics, in which the averaged speed of an apex at $j$-th point ($j = 1, 2, 3$) has an outward velocity $v = v(\varphi_i/2)$ directed along the bisector, but having a general form (not necessarily $2\cos\varphi/2$, as in the case of CHASE ).

We write $\alpha = \varphi_1/2$, $\beta = \varphi_2/2$, $\gamma = \varphi_3/2$. As above, we find that

$$\dot{\alpha} = \frac{1}{\sin\beta}(v(\gamma)\sin\gamma - v(\alpha)\sin\alpha) + \frac{1}{\sin\gamma}(v(\beta)\sin\beta - v(\alpha)\sin\alpha). \tag{5}$$

Denote $g(\alpha) = v(\alpha)\sin\alpha$. Then, the condition on the stationary point obtains the form

$$g(\alpha) = g(\beta) = g(\gamma).$$

Differentiating (5) with respect to $\alpha$ and $\beta$, we obtain linear stability conditions on stationary point. Let $J = (J_{i,j})$ be the linear part of (5). The linear stability conditions then have the form

$$0 \geqslant \operatorname{tr}(J) = -\left(\frac{g'(\alpha)(\sin\beta+\sin\gamma)}{\sin\beta\sin\gamma} + \frac{g'(\beta)(\sin\alpha+\sin\gamma)}{\sin\alpha\sin\gamma} + \frac{g'(\gamma)(\sin\beta+\sin\alpha)}{\sin\beta\sin\alpha}\right)$$

and

$$0 \leqslant \det(J) = \frac{(g'(\alpha)g'(\beta)+g'(\beta)g'(\gamma)+g'(\gamma)g'(\alpha))(\sin\alpha+\sin\beta+\sin\gamma)}{\sin\alpha\sin\beta\sin\gamma}.$$

In particular, if $g'(\pi/3) > 0$, then the regular triangles are stable.

## 5 Conclusions

### 5.1 Summary

Summarizing, the results we presented lend theoretical support to the experimentally observed phenomena: The CHASE dynamics, which is approximating the original Markov chain well for large polygons near $k$-sided regular ones for $k \geqslant 5$, is unstable. Although we do not know what is the correct approximation for polygons close (in some sense) to large triangles, a reasonable CHASE -like approximation is stable near regular triangles. The problem of *proving* the asymptotic symmetry breaking remains open.

### 5.2 Higher dimensions

One can look at the analogous problem in higher-dimensional setting. Experiments show that the convex hulls of RRTs in $\mathbb{R}^d$ form approximately a regular $d$-simplex. We do not have, yet, any results similar to our planar case.

### 5.3 Case $k \to \infty$

One can try to approximate the evolution of convex hull of the RRT near the acute angle in a more refined way by considering the limiting case of CHASE for the infinitely many vertices for the initial shape. Without going into details, we just remark here, that in a natural parametrization, the CHASE evolution is described in this limit by the one-dimensional Boussinesq equation

$$\dot{\varphi} = (\varphi^2)''.$$

.

## References

1. Yu. Baryshnikov and V. Zharnitsky. Sub-Riemannian geometry and periodic orbits in classical billiards. *Math. Res. Lett.*, 13(4):587–598, 2006.

2. M. Ballerini et al. Interaction ruling animal collective behavior depends on topological rather than metric distance: Evidence from a field study. *Proc. National Academy of Sciences*, 105:1232–1237, 2008.
3. J. Glover, D. Rus, N Roy, and G. Gordon. Robust models of object geometry. In China Beijing, editor, *Proceedings of the IROS Workshop on From Sensors to Human Spatial Concepts*, 2006.
4. D. Hsu, L. E. Kavraki, J.-C. Latombe, R. Motwani, and S. Sorkin. On finding narrow passages with probabilistic roadmap planners. In P. Agarwal et al., editor, *Robotics: The Algorithmic Perspective*, pages 141–154. A.K. Peters, Wellesley, MA, 1998.
5. D. Hsu, J.-C. Latombe, and R. Motwani. Path planning in expansive configuration spaces. *International Journal Computational Geometry & Applications*, 4:495–512, 1999.
6. S. Karaman and E. Frazzoli. Sampling-based algorithms for optimal motion planning. *International Journal of Robotics Research*, 30(7):846–894, 2011.
7. D.G. Kendall, D. Barden, T.K. Carne, and H. Le. *Shape and Shape Theory.* John Wiley and Sons, 1999.
8. Allen Knutson. The symplectic and algebraic geometry of Horn's problem. *Linear Algebra Appl.*, 319(1-3):61–81, 2000.
9. H. J. Kushner and G. G. Yin. *Stochastic Approximation and Recursive Algorithms and Applications*. Springer Verlag, 2003.
10. F. Lamiraux and J.-P. Laumond. On the expected complexity of random path planning. In *Proceedings IEEE International Conference on Robotics & Automation*, pages 3306–3311, 1996.
11. S. M. LaValle. Rapidly-exploring random trees: A new tool for path planning. TR 98-11, Computer Science Dept., Iowa State University, October 1998.
12. S. M. LaValle. Robot motion planning: A game-theoretic foundation. *Algorithmica*, 26(3):430–465, 2000.
13. S. M. LaValle. *Planning Algorithms*. Cambridge University Press, Cambridge, U.K., 2006. Also available at http://planning.cs.uiuc.edu/.
14. O. Nechushtan, B. Raveh, and D. Halperin. Sampling-diagram automata: A tool for analyzing path quality in tree planners. In *Proceedings Workshop on Algorithmic Foundations of Robotics*, Singapore, December 2010.
15. H. Robbins and S. Monro. A stochastic approximation method. *Ann. Math. Statistics*, 22:400–407, 1951.
16. J. Yu, D. Liberzon, and S. M. LaValle. Rendezvous wihtout coordinates. *IEEE Transactions on Automatic Control*, 57(2):421–434, 2012.